

© The Author(s), 2022. Published by Cambridge University Press for the Arizona Board of Regents on behalf of the University of Arizona. This is an Open Access article, distributed under the terms of the Creative Commons Attribution-NonCommercial-ShareAlike licence (<http://creativecommons.org/licenses/by-nc-sa/4.0/>), which permits non-commercial re-use, distribution, and reproduction in any medium, provided the same Creative Commons licence is used to distribute the re-used or adapted article and the original article is properly cited. The written permission of Cambridge University Press must be obtained prior to any commercial use.

RECENT SPATIAL DISTRIBUTION OF RADIOCARBON IN URBAN TREE LEAVES AT GYEONGJU, SOUTH KOREA

Sang-Hun Lee¹  • Min-Ji Kong²  • Seung-Gyu Lee¹ • Sae-Hoon Park¹ • Yu-Seok Kim^{1*} 

¹Division of Creative Convergence Engineering, Dongguk University, 123, Dongdae-ro, Gyeongju-si, Gyeongsangbuk-do, 38066, South Korea

²Conservation Science Division, NRICH, 132 Munji-ro, Yuseong-gu, Daejeon, 34122, South Korea

ABSTRACT. Radiocarbon (^{14}C) in natural samples undergoes changes due to variations in atmospheric CO_2 resulting from anthropogenic activities. To analyze the variation of the ^{14}C ratio in atmospheric CO_2 , deciduous tree leaves were collected in Gyeongju, a popular tourist city in South Korea. Leaf samples were collected from *Prunus* subg. *Cerasus* trees at five different sampling points throughout the city over 3 years (2018, 2020, and 2021). The ^{14}C data of the samples were categorized into three groups (downtown, rural, and tourist sites) and analyzed for variations among the different years. The ^{14}C ratio at downtown sites was stable after 2018, the rural site ratio increased between 2018 and 2020 and then decreased between 2020 and 2021, and the tourist site ratio increased after 2018. We theorize that the increased ^{14}C ratio at the tourist site was caused by a decrease in tourism after 2018.

KEYWORDS: AMS, carbon dioxide, fossil fuel, leaf, radiocarbon.

INTRODUCTION

Radiocarbon (^{14}C) is produced in the stratosphere by cosmic rays, which consist of high-energy protons and helium nuclei (Adriani et al. 2011). Cosmic rays are transformed to neutrons by interaction with gases (mostly ^{14}N) in the atmosphere, which produces ^{14}C on the Earth (Lal and Jull 2001). The global production rate of ^{14}C in the atmosphere is 1.8–2.5 atoms per second per cm^2 (Mak et al. 1999). The ^{14}C is oxidized to ^{14}CO , which is further oxidized to $^{14}\text{CO}_2$ by hydroxyl radicals (Pandow et al. 1960; Demidov and Markelov 2005; Hajdas et al. 2021). Until 1890, the ^{14}C content was only affected by the amount of cosmic rays from the Earth and solar cycle. However, anthropogenic activities became an influencing factor of ^{14}C content after 1890. Changes in the $^{14}\text{C}/^{12}\text{C}$ ratio under anthropogenic influence were measured during 1890–1945 (Suess 1955); thus, the decreasing $^{14}\text{C}/^{12}\text{C}$ in the atmosphere due to fossil fuel usage was named the Suess effect. This ratio increased from 1955 to 1965 due to nuclear weapon testing and production, with a maximum value recorded in 1963 in the Northern Hemisphere, after which it declined (Levin et al. 2010). The ^{14}C concentration has gradually decreased and now resembles that before 1955 (Levin et al. 2013). In the modern age, natural events and anthropogenic influences cause ^{14}C ratio fluctuations. At the local scale, a primary reason for fluctuations in ^{14}C content is the consumption of fossil fuels. The ^{14}C isotope can be used as a powerful tool for tracking fossil carbon (Zhang et al. 2021). Plants capture atmospheric carbon via photosynthesis, thus extracting radiocarbon from CO_2 in the atmosphere (Pazdur et al. 2007). Similarly, tree rings have been used to interpret fossil carbon from the atmosphere at the local scale (Hou et al. 2020). Additionally, deciduous trees and grasses absorb CO_2 from the atmosphere; their leaves can represent the atmospheric $^{14}\text{C}/^{12}\text{C}$ ratio at the time when they were alive at sites affected by fossil fuel usage (Park et al. 2015; Ndeye et al. 2017; Varga et al. 2019; Sharma et al. 2023).

*Corresponding author. Email: unison@dongguk.ac.kr



In this study, variations in the ^{14}C ratio were measured in the well-known tourist city of Gyeongju in South Korea to determine the Suess effect. The deciduous leaves were collected from rural and urban areas of the city in 2018, 2020, and 2021. The samples were prepared and measured using an accelerator mass spectrometer (AMS) at Dongguk University (Lee et al. 2020a).

MATERIALS AND METHODS

Sampling Sites and Samples

South Korea is located in northeast Asia and experiences the Asian monsoon. In winter, cold and dry winds blow from Siberia, while in summer, hot and moist winds blow from tropical areas. The average temperature is 25°C with a total annual rainfall of approximately 1500 mm, 50%–60% of which occurs in summer (Korean Meteorological Association, <http://weather.go.kr> [December 10, 2020]). Gyeongju has a population of approximately 240,000 and consists of a small industrial facility, vast agricultural lands, and famous tourist attractions. The residential area of Gyeongju is concentrated in a narrow zone, while the rest of the area is devoted to agriculture. Hence, we considered that most CO₂ content was contributed by citizen and tourist economic activities like transportation, not industrial facilities, that consumed fossil fuels. The distance from the small industrial facility to the downtown sites were up to 3 km, 7 km to the tourist site, and 20 km to the rural site. The nuclear power plant in Gyeongju is located up to 24 km away from the sampling sites; the ^{14}C effect from the nuclear power plant is discussed in the Results and Discussion section. To examine the fossil carbon content, five sites at rural, downtown, and tourist locations were selected, and leaves from *Prunus* subg. *Cerasus*, a local deciduous tree, were collected in 2018, 2020, and 2021. From these five sites, 25 samples were collected followed by chemical pretreatment; however, only 15 of these samples were measured considering sample condition after pretreatment. These excepted samples became very low mass less than 1 mg after pretreatment. We decided to exclude these samples for the accuracy of measurement. The sample codes are in double-digits, where the first number denotes the year of collection (0: 2018, 1: 2020, 2: 2021), while the second number denotes the site type (1: rural, 2: tourist, 3–5: downtown) (Table 1, Figure 1). The population density of the downtown area was >10,000 people/km², while the rural site had a lower density of 1,000 people/km². The tourist site was selected based on the number of tourists per year, which was >5,000,000.

Chemical Pretreatment and Graphitization

The leaves were chemically pretreated using as an acid-base-acid method to clean the surface and remove any contaminants (Brock et al. 2010). After pretreatment, the samples were dried at 60°C for 2 hr, followed by combustion in an Element Analyzer (FlashSmart, ThermoFisher Scientific, USA) at 1800°C to convert the carbon in the samples to CO₂ (Aertz-Bijma et al. 2001). The CO₂ gas was trapped in the graphitization system installed at Dongguk University (Lee et al. 2020b). The gas was transferred to the reactor at –20°C through a vacuum line at low pressure (10^{-5} mbar), while H₂O was trapped by low temperature in the CO₂ trap line. Pure CO₂ gas was reacted with iron powder and H₂ at 550°C for approximately 3 hr, generating graphite powder along with iron. The graphite samples were pressed into an aluminum cathode using a pneumatic sample press (Ionplus AG, Switzerland) to measure the carbon isotope ratio (Lee et al. 2020a, 2020b).

Table 1 Sampled tree species, location, and time (year-month) of sampling in Gyeongju, South Korea.

Sample code	Description	Latitude	Longitude	Year-month
01	Rural	35° 45' 27.3" N	129° 02' 49.6" E	2018-09
02	Tourist	35° 50' 03.7" N	129° 17' 14.1" E	2018-09
03	Downtown1	35° 50' 43.2" N	129° 12' 49.3" E	2018-09
04	Downtown2	35° 50' 29.6" N	129° 12' 18.0" E	2018-09
05	Downtown3	35° 52' 19.4" N	129° 13' 09.4" E	2018-09
11	Rural	35° 45' 27.9" N	129° 02' 49.1" E	2020-07
12	Tourist	35° 50' 05.4" N	129° 17' 15.0" E	2020-07
13	Downtown1	35° 50' 49.4" N	129° 12' 57.6" E	2020-07
14	Downtown2	35° 50' 49.0" N	129° 12' 20.3" E	2020-07
15	Downtown3	35° 52' 20.1" N	129° 13' 09.0" E	2020-07
21	Rural	35° 45' 16.9" N	129° 02' 48.0" E	2021-07
22	Tourist	35° 50' 03.6" N	129° 17' 14.0" E	2021-07
23	Downtown1	35° 50' 42.2" N	129° 12' 58.3" E	2021-07
24	Downtown2	35° 50' 30.3" N	129° 12' 17.4" E	2021-07
25	Downtown3	35° 52' 20.1" N	129° 13' 07.3" E	2021-07

Measurements and Calculations

The samples were measured using a MICADAS accelerator mass spectrometer at Dongguk University (Lee et al. 2020a). Oxalic Acid II (NIST-SRM 4990C) samples and IAEA-C1 samples were measured to normalize sample data and check the background of the AMS. The sample data were reduced using the BATS program (Wacker et al. 2010), which calculates the radiocarbon unit, $\delta^{13}\text{C}$, $F^{14}\text{C}$, radiocarbon age, and calendar age, but does not calculate $\Delta^{14}\text{C}$. Carbon isotopes of the leaves are affected by mass fractionation and must be normalized with respect to a standard. The $F^{14}\text{C}$ unit is the ratio of leaf sample ^{14}C activity and standard material (Ox-I) ^{14}C activity, which we changed to a ratio $(^{14}\text{C}/^{12}\text{C})$. However, this unit does not represent the ^{14}C decay of the standard sample from 1950. The $\Delta^{14}\text{C}$ unit represents mass fractionation and radioactive decay, the following equation from Stuiver and Polach (1977) was used:

$$\Delta^{14}\text{C} (\%) = \left(\frac{\frac{^{14}\text{C}}{^{12}\text{C}}|_{\text{sample}, -25} \times e^{\left(\frac{1950-y}{8267}\right)}}{0.7459 \left(\frac{^{14}\text{C}}{^{12}\text{C}}\right)^2|_{\text{oxII}, -25}} - 1 \right) \times 1000\% \quad (1)$$

where $^{14}\text{C}/^{12}\text{C}|_{\text{sample}}$ is the value of the measured sample and $^{14}\text{C}/^{12}\text{C}|_{\text{oxII}}$ is the value of the standard sample (SRM 4990C). The BATS program was used to verify the precision of the measured data. Thus, the $\Delta^{14}\text{C}$ values were calculated from the $^{14}\text{C}/^{12}\text{C}$ data.

RESULTS AND DISCUSSION

An increase in the $\Delta^{14}\text{C}$ values from 2018 to 2021 was observed. The average $\Delta^{14}\text{C}$ values were $-25.1 \pm 2.0\%$ in 2018, $-20.7 \pm 2.0\%$ in 2020, and $-18.4 \pm 3.0\%$ in 2021, indicating an increase each year. The complete dataset for all 3 years ranged from -32.0% to -6.9% . The minimum value was seen at the Downtown 1 site in 2018, while the maximum value was seen at the tourist site in 2021. Table 2 shows the overall AMS measurement results for the tree leaves.

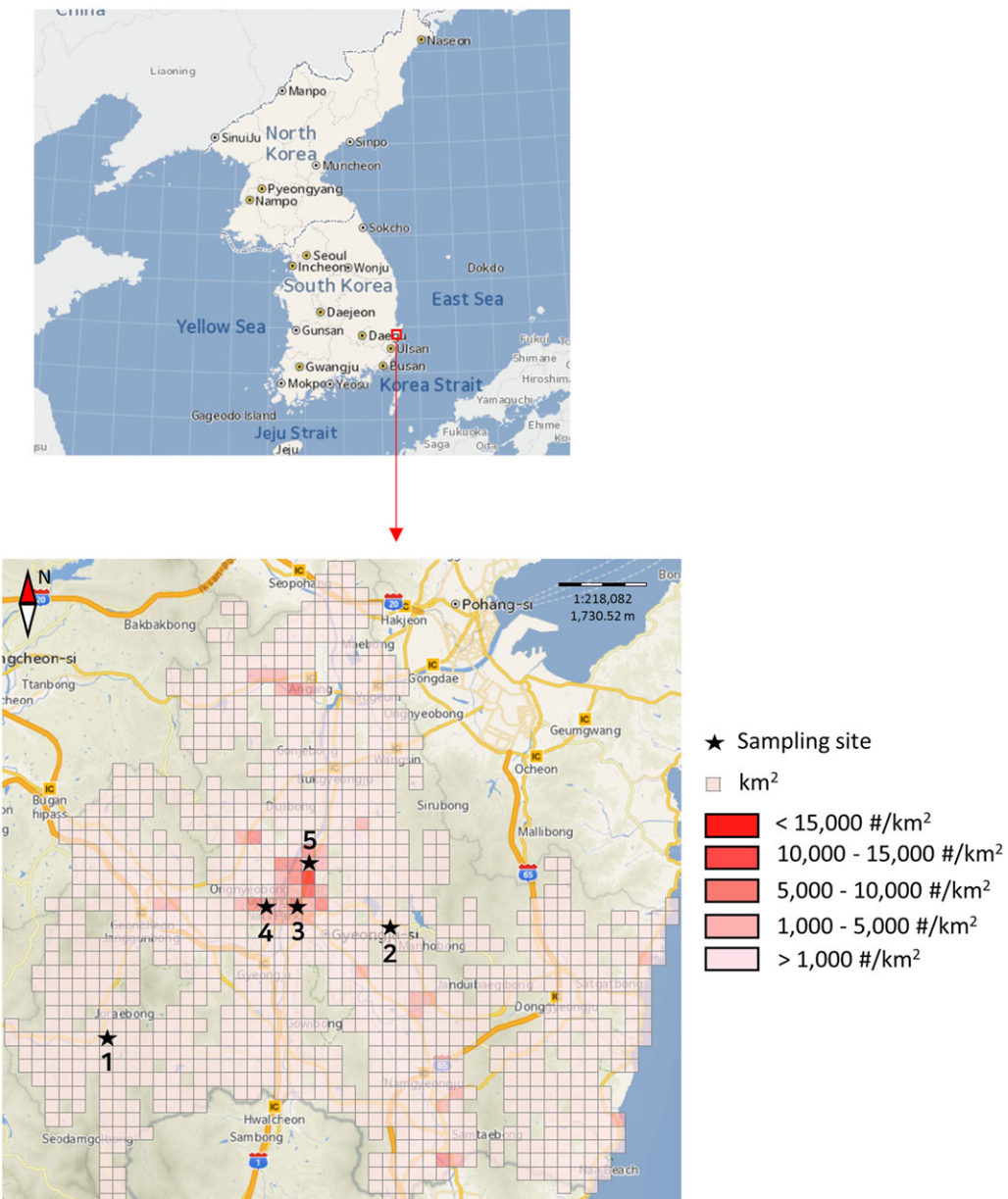
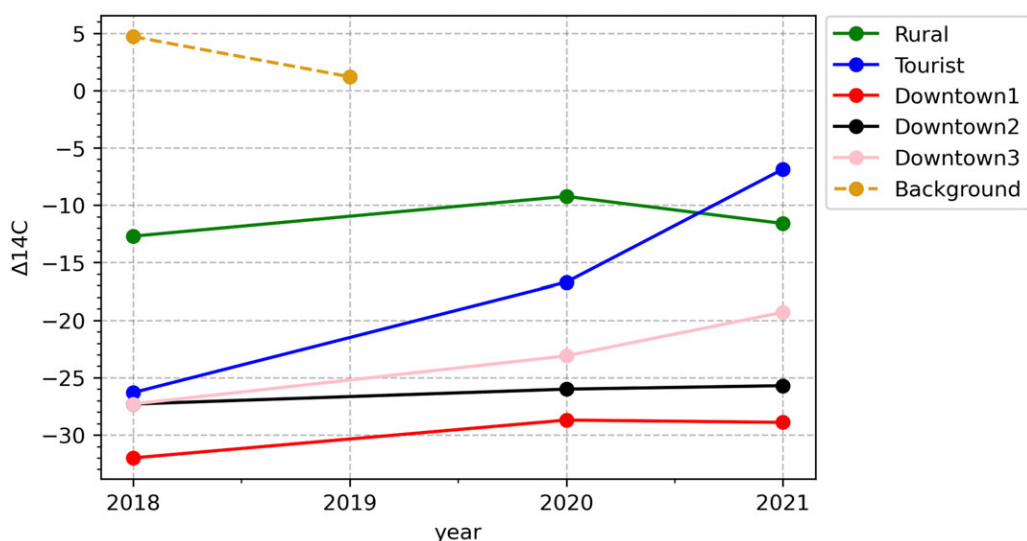


Figure 1 Sites of sampling points with their population density (as of October 2018).

The sample value from the tourist site increased by 36.4% between 2018 and 2020 and 59.0% between 2020 and 2021. The rural site value increased by 27.3% between 2018 and 2020 and was stable between 2020 and 2021. The downtown 1 and downtown 2 site values were stable for 4 years, while the downtown 3 site value increased by 15.3% between 2018 and 2020 and was stable between 2020 and 2021. Next, the ^{14}C ratio data at Gyeongju was compared with that of Jungfraujoch, Switzerland (Emmenegger et al. 2021). The measured ^{14}C ratio of Jungfraujoch was greater than 0, and the values decreased between 2018 and 2019. The differences in these

Table 2 Annual $\Delta^{14}\text{C}$ data of the leaves from Gyeongju, South Korea by year and sample site.

Sample code	Collection year	Site character	$\Delta^{14}\text{C}$ (‰)	Average for time (‰)
01	2018	Rural	-12.7 ± 2.0	
02	2018	Tourist	-26.3 ± 2.0	
03	2018	Downtown1	-32.0 ± 2.0	
04	2018	Downtown2	-27.3 ± 2.0	
05	2018	Downtown3	-27.3 ± 2.0	
11	2020	Rural	-9.2 ± 2.0	-20.7 ± 2.0
12	2020	Tourist	-16.7 ± 2.0	
13	2020	Downtown1	-28.7 ± 2.0	
14	2020	Downtown2	-26.0 ± 2.0	
15	2020	Downtown3	-23.1 ± 2.0	
21	2021	Rural	-11.6 ± 3.0	-18.4 ± 3.0
22	2021	Tourist	-6.9 ± 3.0	
23	2021	Downtown1	-28.9 ± 3.0	
24	2021	Downtown2	-25.7 ± 3.0	
25	2021	Downtown3	-19.3 ± 3.0	

Figure 2 $\Delta^{14}\text{C}$ (‰) values of all tree leaf samples and fresh air data of Jungfraujoch (as background).

results indicate that the increase in the ^{14}C ratio at Gyeongju was influenced by anthropogenic factors; the variation in the results is shown in Figure 2. The ^{14}C ratio is indicated by the green line for the rural site, blue line for the tourist site, red line for downtown 1, black line for downtown 2, pink line for downtown 3 sites, and a yellow line for the Jungfraujoch (as background).

A possible explanation for decreasing $\Delta^{14}\text{C}$ values in small areas is ^{14}C -free carbon released into the atmosphere from fossil fuel combustion (Turnbull et al. 2017).

The average ^{14}C ratio in the city was increased from $-28.8 \pm 2.0\text{\textperthousand}$ in 2018 to $-25.9 \pm 2.0\text{\textperthousand}$ in 2020. The increase could be affected by a decrease in car mileage in the city from 38.7 km/day in 2018 to 37.5 km/day in 2020 (Korea Transportation Safety Authority. <http://www.kotsa.or.kr> [December 10, 2020]). With a higher population density ($>10,000 / \text{km}^2$) than the rural and tourist sites, the downtown sites had lower $\Delta^{14}\text{C}$ values. One explanation for the significant increase in the ^{14}C ratio at the tourist site was the reduction in the number of tourists after 2019 due to the COVID-19 pandemic; the monthly numbers decreased by 16% in 2020 and 8% in 2021 compared to 2019 (Korea Tourism Organization. Visit Korea. <https://datalab.visitkorea.or.kr> [December 10, 2020]), and the total numbers decreased after 2019. The population density of the tourist site was similar to that of the rural site; however, the ^{14}C ratio of the tourist site was lower than that of the rural site in 2018 and 2020. Nevertheless, the ^{14}C ratio was higher at the tourist site in 2021 compared to the rural site despite a slight change in the population density. The variation in ^{14}C content in the tourist site was mainly attributed to the decreased intensity of traffic connected to tourism. The ^{14}C ratio of the downtown 1 and 2 sites was lower than that of the downtown 3 site because they are closer to a new tourist site called Hwang-ri-dan-gil in Gyeongju, which has been experiencing an increase in the number of visitors since 2018. In this study, samples were collected up to 24 km from the Wolsung nuclear power plant. Nearly all ^{14}C from the power plant was deposited within a 2 km radius (Kim et al. 2000). In addition, the distribution of ^{14}C from nuclear power plants is influenced by geography, in combination with distance and meteorology. Tree samples were measured by Dongguk University and the ^{14}C was blocked by To-ham Mountain (700 m height), which is located between the sampling site and the nuclear power plant (Lee et al. 2021). The distribution of ^{14}C from nuclear power plants and its dependence on geography will be studied in the future. In addition, we aim to investigate the variations in ^{14}C ratios in the study area based on tree-rings in follow-up research.

CONCLUSION

Fifteen samples from five different locations were measured in the region of Gyeongju, South Korea over 3 years (2018, 2020, and 2021), covering several industrial facilities, small residential sites, vast agricultural lands, and famous tourist sites. We studied the fossil carbon load of trees derived from three different types of areas: downtown, rural, and tourist sites. The city $\Delta^{14}\text{C}$ average levels in the sampled tree leaves were $-25.1 \pm 2.0\text{\textperthousand}$ in 2018, $-20.7 \pm 2.0\text{\textperthousand}$ in 2020, and $-18.4 \pm 3.0\text{\textperthousand}$ in 2021, showing a gradual increase each year. A possible explanation for this increase is a decrease in daily car mileage from 38.7 km in 2018 to 37.5 km in 2020. At densely populated sites, the $\Delta^{14}\text{C}$ level was $-26.4 \pm 2.0\text{\textperthousand}$, compared to the higher values from rural and tourist sites ($-11.1 \pm 2.0\text{\textperthousand}$ and $-16.6 \pm 2.0\text{\textperthousand}$, respectively). The $\Delta^{14}\text{C}$ of the tourist site increased from $-26.3 \pm 2.0\text{\textperthousand}$ in 2018 to $-6.9 \pm 3.0\text{\textperthousand}$ in 2021. The significant increase at the tourist site may be affected by decreasing tourist numbers and reduced car mileage after 2019. In addition, we speculate that fossil carbon emissions were significantly affected by the pandemic situation after 2020. In the future, studies will be conducted on ^{14}C in tree rings to further understand the carbon variability.

ACKNOWLEDGMENTS

This work was supported by the National Research Foundation of Korea (NRF) grant funded by the Korea government (MSIT) (No.2022R1A2C2006213).

REFERENCES

- Adriani O, Barbarin GC, Bazilevskaya GA, Bellotti R, Boezio M, Bogomolov EA, Bonechi L, Bongi M, Bonvicini V, Borisov S, Bottai S. 2011. PAMELA measurements of cosmic-ray proton and helium spectra. *Science* 322(6025):69–72.
- Aertz-Bijma AT, van der Plicht J, Meijer HAJ. 2001. Automatic AMS sample combustion and CO₂ collection. *Radiocarbon* 43(2A):293–298.
- Brock F, Higham T, Ditchfield P, Ramsey CB. 2010. Current pretreatment methods for AMS radiocarbon dating at the oxford radiocarbon accelerator unit (ORAU). *Radiocarbon* 52(1):103–112.
- Demidov AI, Markelov IA. 2005. Thermodynamics of reaction of carbon with oxygen. *Russian Journal of Applied Chemistry* 78(5):707–710.
- Emmenegger L, Leuenberger M, Steinbacher M, ICOS RI. 2021. ICOS ATC/CAL ¹⁴C Release, Jungfraujoch (10.0 m), 2016-01-04-2019-08-11. URL: <https://hdl.handle.net/11676/JmhH4pUyWlbqTAAx4x54deg>.
- Hajdas I, Ascough P, Garnett MH, Fallon SJ, Pearson CJ, Gianluca Q, Kirsty LS, Yamaguchi H, Yoneda M. 2021. Radiocarbon. *Nature Reviews Methods Primers* 1(1):1–26.
- Hou Y, Zhou W, Cheng P, Xiong X, Du H, Niu Z, Yu X, Fu Y, Lu X. 2020. ¹⁴C-AMS measurements in modern tree rings to trace local fossil fuel-derived CO₂ in the greater Xi'an area, China. *Science of the Total Environment* 715:136669.
- Kim CK, Lee SK, Rho BH, Lee YG. 2000. Environmental distribution and behavior of ³H and ¹⁴C around Wolsung nuclear power plants. *Health Physics* 78(6):693–9.
- Lal D, Jull AJT. 2001. In-situ cosmogenic ¹⁴C: production and examples of its unique applications in studies of terrestrial and extraterrestrial processes. *Radiocarbon* 43(2B):731–742.
- Lee SH, Hwang MJ, Jang JH, Choi JS, Kim YS. 2021. A study on the measurement of C-14 of tree samples around Wolseong Nuclear Power Plant. *Journal of Radiation Protection and Research Autumn Meeting*.
- Lee SH, Park SH, Kong MJ, Kim YS. 2020a. A new compact AMS facility at the Dongguk University. *Nuclear Instruments and Methods in Physics Research B* 465:15–8.
- Lee SH, Kang DU, Lee JB, Kim MJ, Park SH, Kim YS. 2020b. Evaluation of acid-alkali-acid pretreatment for environmental wood samples at Dongguk University. *Transactions of the Korean Nuclear Society Virtual Autumn Meeting*.
- Levin I, Naegler T, Kromer B, Diehl M, Francey RJ, Gomez-Pelaez AJ, Steele LP, Wagenbach D, Weller R, Worthy DE. 2010. Observations and modelling of the global distribution and long-term trend of atmospheric ¹⁴CO₂. *Tellus B* 62(1):26–46.
- Levin I, Kromer B, Hammer S. 2013. Atmospheric $\Delta^{14}\text{CO}_2$ trend in Western European background air from 2000 to 2012. *Tellus B* 65(1):20092.
- Mak J, Brenninkmeijer C, Southon J. 1999. Direct measurement of the production rate of ¹⁴C near Earth's surface. *Geophysical Research Letters* 26(22):3381–3384.
- Ndeye M, Sene M, Diop D, Saliege JF. 2017. Anthropogenic CO₂ in the Dakar (Senegal) urban area deduced from ¹⁴C concentration in tree leaves. *Radiocarbon* 59(3):1009–1019.
- Pandow M, MacKay C, Wolfgang R. 1960. The reaction of atomic carbon with oxygen: Significance for the natural radio-carbon cycle. *Journal of Inorganic and Nuclear Chemistry* 14(3-4):153–158.
- Park JH, Hong W, Xu X, Park G, Sung KS, Sung K, Lee J, Nakanishi T, Park H. 2015. The distribution of $\Delta^{14}\text{C}$ in Korea from 2010 to 2013. *Nuclear Instruments and Methods in Physics Research B* 361:609–613.
- Pazdur A, Nakamura T, Pawelczyk S, Pawlyta J, Piotrowska N, Rakowski A, Sensula B, Szczepanek M. 2007. Carbon isotopes in tree rings: climate and Suess effect interferences in the last 400 years. *Radiocarbon* 49(2):775–788.
- Sharma R, Kunchala RK, Ojha S, Kumar P, Gargari S, Chorpa S. 2023. Spatial distribution of fossil fuel derived CO₂ over India using radiocarbon measurements in crop plants. *Journal of Environmental Science* 124:19–30.
- Stuiver M, Polach HA. 1977. Discussion reporting of ¹⁴C ages. *Radiocarbon* 19(3):355–363.
- Suess HE. 1955. Radiocarbon concentration in modern wood. *Science* 122(3166):415–417.
- Turnbull JC, Keller ED, Norris MW, Wiltshire RM. 2017. Atmospheric monitoring of carbon capture and storage leakage using radiocarbon. *International Journal of Greenhouse Gas Control* 56:93–101.
- Varga T, Barnucz P, Major I, Lisztés-Szabó Z, Jull AJT, Laszlo E, Penezes J, Molnar M. 2019. Fossil carbon load in urban vegetation for Debrecen, Hungary. *Radiocarbon* 61(5):1199–210.
- Wacker L, Christl M, Synal HA. 2010. BATS: A new tool for AMS data reduction. *Nuclear Instruments and Methods in Physics Research B* 268(7–8):976–979.
- Zhang Y, Jin Z, Sikand M. 2021. The top-of-atmosphere, surface and atmospheric cloud radiative kernels based on ISCCP-H datasets: method and evaluation. *Journal of Geophysical Research: Atmospheres* 126(44):1–34.